Magnetic properties of $LaFe_{1-x}Cr_xO_3$ and $Fe_{2-2x}Cr_{2x}O_3$ mixed oxides

E. Loudghiri[1], A. Belayachi[1*], M. Nogues[2], M. Taibi[3], A. Dahmani[1,3], M. EL Yamani[1] and J. Aride[3]
[1]*Laboratoire de Physique des Matériaux, Faculté des Sciences Université Mohammed V, B.P. 1014 Rabat, Maroc*
[2]*Laboratoire de Magnétisme et d'Optique de l'Université de Versailles (URA 1531), Batiment Fermat, 45 Avenue des Etats Unis, 78035 Versailles Cedex, France.*
[3]*Laboratoire de Physico-Chimie des Matériaux associé à l'AUF (LAF 502), Ecole Normale Supérieure Takadoum B.P. 5118 Rabat Maroc.*

Mixed oxides with formula $LaFe_{1-x}Cr_xO_3$ and $Fe_{2-2x}Cr_{2x}O_3$, where $0 \le x \le 1$, are studied. The samples have been prepared using solid state reaction technique in air. The X-ray diffraction spectra indicated that the samples crystallize in a corundum phase with space group (R3c) for $Fe_{2-2x}Cr_{2x}O_3$ and in the perovskite structure for $LaFe_{1-x}Cr_xO_3$. Many techniques have been used to explore the magnetic properties of the systems. High field, ZFC and FC magnetization vs. temperature, d.c. susceptibility and Mössbauer spectroscopy were carried out. High temperature magnetic susceptibility measurements and high field magnetic magnetization (H $\le$ 20 T) show that the behavior of the susceptibility and the magnetization are complex. Mössbauer spectra of the solid solutions have been measured at 4.2 K and in the temperature range 77 K to 300 K. The shapes of spectra are unusual, showing strong relaxation phenomena in a wide temperature range as recently observed for many frustrated systems. The results are discussed by establishing the existence of various magnetic structures, inducing intermediate magnetic phases between the antiferromagnetic and the paramagnetic states. Preliminary magnetic phase diagrams of the systems have been established.

I. INTRODUCTION

The competition of several kinds of magnetic order leads to a great variety of disorder phenomena in the magnetic properties of randomly mixed crystals of two components.[1-9] The compounds with general formula ABO_3 where A is lanthanum La, B is Fe or Cr, are perovskite with orthorhombic deformation. The basic $LaFeO_3$ and $LaCrO_3$ show antiferromagnetic structure, with type G, where each ion has six antiparallel nearest neighbors. The Néel temperatures are approximately 750 K and 280 K respectively. In previous works, we have shown the existence of non-collinear antiferromagnetic structure for $LaFe_{1-x}Cr_xO_3$.[10,11] Cr_2O_3 and α-Fe_2O_3 have the corundum structure. Many investigations have been reported on the study of magnetic properties of chromium oxide Cr_2O_3 and iron oxide α-Fe_2O_3. R. Street and B. Lewis[12] found an anomalous variation of the young's modulus near the Néel temperature. The observed change of modulus is caused by a modification of the binding energy versus ionic distance curve produced by the disappearance of magnetic ordering forces at the Néel temperature. High field antiferromagnetic resonance and static magnetic susceptibility have been made on single crystal of Cr_2O_3 by S. Foner[13], which demonstrate the existence of non zero value of the parallel susceptibility at low field. G.W. Pratt and P.T. Baily[14] have explained this behavior by assuming that the Cr spin is canted. A neutron powder study confirm this moment chromium configuration, but perpendicular component of the magnitude required by the canted model does not exhibit long-range order.[15] α-Fe_2O_3 have been investigated by Mössbauer spectroscopy.[16,17] The study shows that α-Fe_2O_3 is an antiferromagnet which shows weak ferromagnetism above T_M = 260 K called Morin temperature. Below T_M the spins point along the [111] direction and above T_M, the spins are perpendicular to the [111] axis.[18] Some studies have been made with non magnetic substitutions for chromium in Cr_2O_3[19-23] and iron in α-Fe_2O_3.[24,25] A spatially modulated spin structure of the conical spiral type was observed for $Fe_{2-2x}Cr_{2x}O_3$ with x>0.7 in neutron scattering measurements on powders.[26] Spin fluctuations have been shown in $Fe_{0.07}Cr_{1.93}O_3$ using Mössbauer spectroscopy.[27] On the other hand, anomalous in temperature dependence of the magnetic moment of $Fe_{2-2x}Cr_{2x}O_3$ for $0.1 \le x \le 0.5$ has been observed and explained by antiparallel orientation of the mean weakly-ferromagnetic moments of Fe^{3+} and Cr^{3+} ions.[28] The present work gives the result of a detailed study performed on both of $LaFe_{1-x}Cr_xO_3$ and $Fe_{2-2x}Cr_{2x}O_3$ solid solution with $0 \le x \le 1$ using magnetization measurements, d.c. magnetic susceptibility and Mössbauer spectroscopy. The synthesis of experimental results allows to the description of magnetic phase diagrams of the mixed systems.

II. EXPERIMENTAL RESULTS

A. SAMPLES PREPARATION AND STRUCTURE

The perovskite samples $LaFe_{1-x}Cr_xO_3$ have been prepared by heating the oxide La_2O_3 with molar mixtures of iron (III) oxide and chromium (III) oxide in air for 72 hours at 1000 °C. At last the samples were annealed under oxygen atmosphere for one day at 1400 °C. The X-ray spectra indicated that the compounds crystallize in the perovskite structure with orthorhombic deformation, their space group is $D_{2h}^{16}(Pbnm)$.[11] Solid solution of the system $Fe_{2-2x}Cr_{2x}O_3$, in powder form, was prepared

* E-mail: belayach@fsr.ac.ma.

from a mixture of high purity oxide powders by heating them at 1300°C in air for 72 h or in oxygen atmosphere for 24 h.

The samples were analyzed with X-ray diffraction using Cuk_α radiation. The lattice parameters a and c were calculated from hexagonal indexing for all compositions. The average calculated lattice parameters are plotted in figures 1 and 2 as function of chromium composition. We note that no Vegard's law is present in this solid solution.

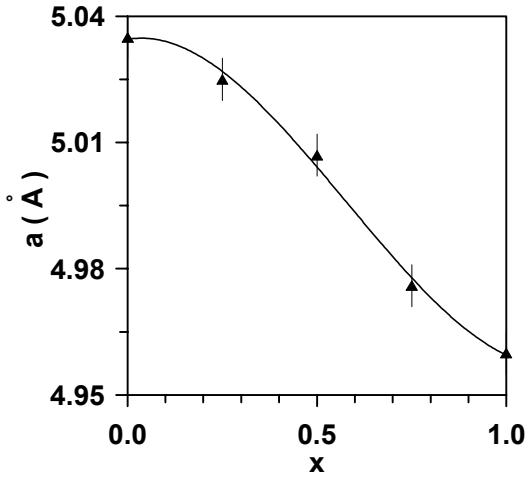

FIG. 1 : Evolution of cell parameter a with Cr^{3+} content.

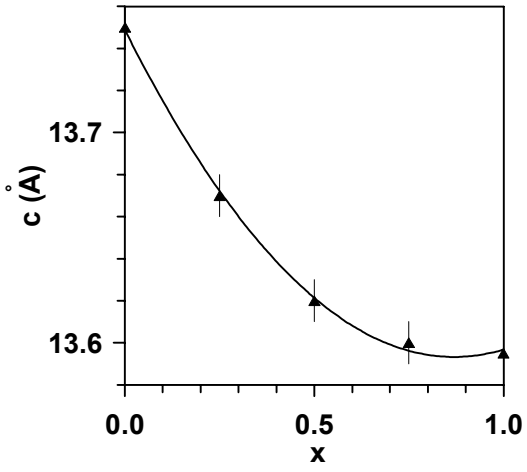

FIG. 2: Evolution of cell parameter c with Cr^{3+} content.

B. MAGNETIZATION MEASUREMENTS

The magnetization measurements were performed with a vibrating sample magnetometer in magnetic field up to 1.8 T, in the temperature range 4.2 K to 300 K. High field magnetization isothermal measurement was performed with axial extraction technique, up to 20 T, of the Service National des Champs Intenses at Grenoble, in the temperature range 4.2 to 300 K.

The high field M-H curves reveal the existence of antiferromagnetic structure superimposed to weak ferromagnetism. For all the samples the magnetization increases linearly with increasing field at all temperatures above a field H_L as presented in figures 3 and 4. The values of H_L depend on the nature of the sample, the concentration of chromium and the temperature. A decrease of H_L with increasing temperature is observed for all the samples. The corrected magnetization M-H curve is obtained by replacing (H,M) in the curve by (H, M-χ_{AF}H), where χ_{AF} is the slope of the isotherm M vs. H for H>H_L. The extrapolation of the linear part of M-H curve to zero gives the saturated magnetization M_{sat} of the weak ferromagnetic moment due to the spin canting. The temperature dependence of the magnetization M_{sat}, for the two systems, is shown in figures 5 and 6.

It seen that for $LaFe_{0.5}Cr_{0.5}O_3$ when the temperature is lowered, M_{sat} shows at first a broad peak and then start decreasing. For $LaFe_{0.25}Cr_{0.75}O_3$ the behavior is different since M_{sat} varies quasi linearly with decreasing temperature, presents a jump near 120 K and increase slowly until 4.2 K.

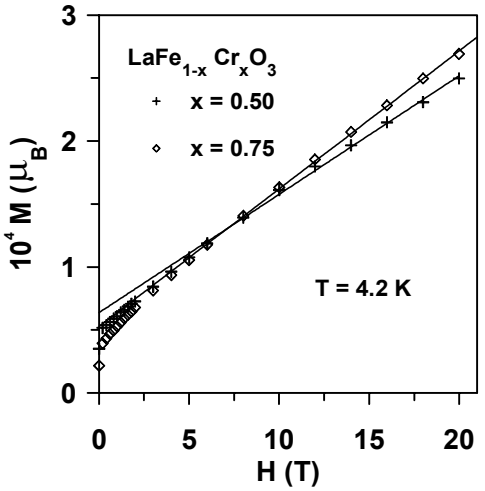

FIG. 3: Magnetization against applied field at 4.2 K for $LaFe_{05}Cr_{05}O_3$ and $LaFe_{025}Cr_{075}O_3$. μ_B denotes the Bohr magneton.

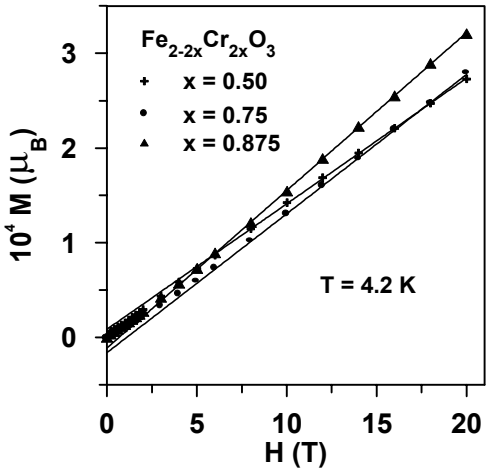

FIG. 4: Magnetization against applied field at 4.2 K for $FeCrO_3$, $Fe_{0.5}Cr_{1.5}O_3$ and $Fe_{0.25}Cr_{1.75}O_3$.

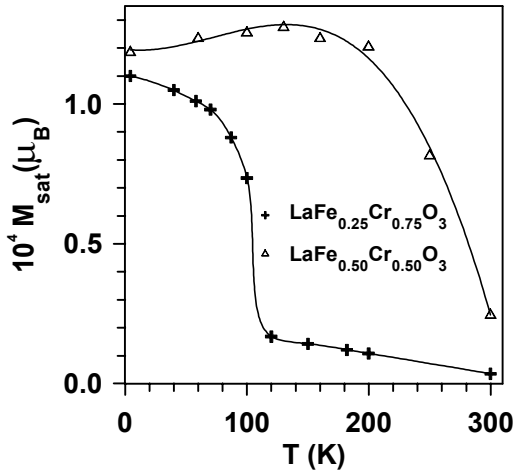

FIG. 5 : Temperature dependence of M_{sat} for $LaFe_{0.5}Cr_{0.5}O_3$ and $LaFe_{0.25}Cr_{0.75}O_3$.

In the case of $Fe_{0.25}Cr_{1.75}O_3$ and $Fe_{0.5}Cr_{1.5}O_3$, the extrapolation of the high slope is negative indicating that the corrected M-H curve obtained by replacing M by M - $\chi_{AF}H$ is reversed whereas this curve is usually positive. For $FeCrO_3$, at first M_{sat} decreases as the temperature increases and becomes negative at T_{comp} which indicate the existence of compensation point in the M_{sat} behavior vs. temperature.

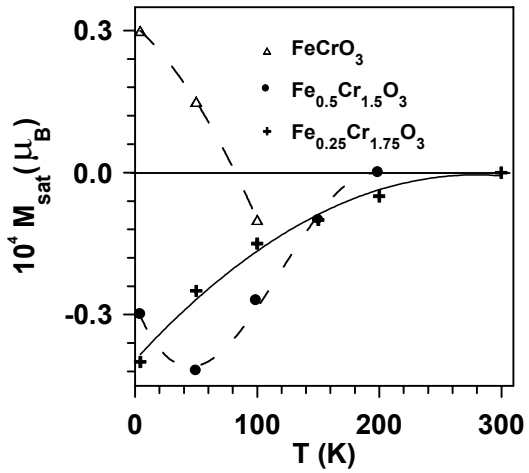

FIG. 6 : Temperature dependence of M_{sat} for $FeCrO_3$, $Fe_{0.5}Cr_{1.5}O_3$ and $Fe_{0.25}Cr_{1.75}O_3$.

C. MAGNETIC SUSCEPTIBILITY

Direct current magnetic susceptibility was measured by a DMS 4 magnetometer in the temperature range 300 K - 900 K under a magnetic applied field of 1 T. The temperature dependence of the inverse molar susceptibility is given in figures 7 and 8. For all the samples a Curie Weiss law is observed at high temperature. The Curie constant determined, in the case of $LaFe_{1-x}Cr_xO_3$ system, is in agreement with that calculated for the spin only state.[10] The results for $Fe_{2-2x}Cr_{2x}O_3$ are summarized in table 1.

x (Cr)	C_{exp}	C_{th}	θ_p
0.25	-	3.52	-
0.5	2.95	3.12	- 1030
0.75	2.75	2.50	- 830
0.875	2.38	2.18	-736

Table 1: Curie constant and the paramagnetic Curie temperature determined by d.c. susceptibility.

The thermal evolution of magnetic susceptibility for $Fe_{2-2x}Cr_{2x}O_3$ depends strongly on the chromium content. The results can be discussed as follow:

For $Fe_{1.5}Cr_{0.5}O_3$, the minimum of $\chi^{-1}_{d.c.}$ vs. T becomes strongly rounded; we note a large plateau in the inverse susceptibility curve. We also can see that the transition from magnetic state to paramagnetism takes place through a large domain of temperature where short-range order obviously exists. For $FeCrO_3$, the minimum of χ^{-1} vs. T exhibits a tendency to a cusp like shape. When x>0.5, a linear variation of the inverse of the susceptibility is observed at high temperature indicating that only paramagnetic regime occurs. With decreasing the temperature, the susceptibility deviates from the Curie Weiss law showing a progressive development of short-range correlation between chromium and iron spins.

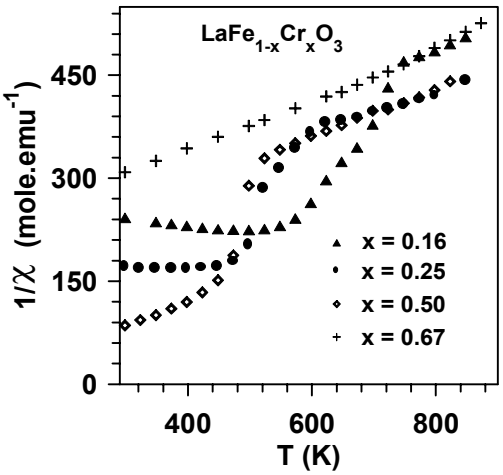

FIG. 7 : Inverse of d.c. susceptibility as function of temperature for the $LaFe_{1-x}Cr_xO_3$ system.

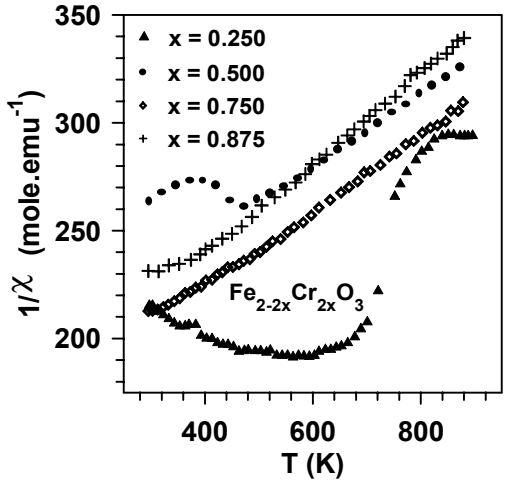

FIG. 8 : Inverse of d.c. susceptibility as function of temperature for the $Fe_{2-2x}Cr_{2x}O_3$ system.

D. MÖSSBAUER EFFECT

Mössbauer spectroscopy experiments were carried out at 4.2 K and above 77 K using a conventional spectrometer operating in the constant acceleration mode. The source used was ^{57}Co in Rh. The isomer shift δ and the quadrupole interaction ε values are typical of trivalent iron ion in octahedral symmetry with tetragonal or trigonal distortion. The small values of the quadrupole splitting show that the electric surrounding of the iron sites are weakly distorted by the introduction of chromium in the cationic matrix, because the similarity of the ionic radii. In addition, a small increase is observed with increasing x for ε. This fact may indicate a very weak increase of the site distortion, as confirmed by the small increase of the experimental line width Γ (Tables 2 and 3).

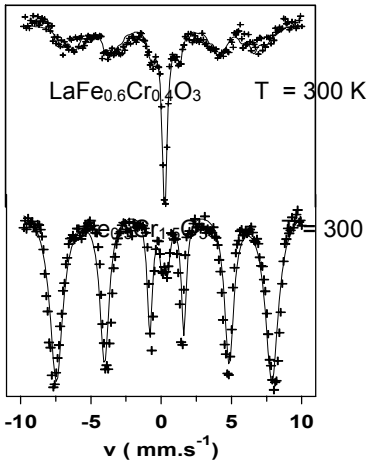

FIG. 9 : Mössbauer spectra at 300 K for the samples $LaFe_{0.6}Cr_{0.4}O_3$ and $Fe_{0.5}Cr_{1.5}O_3$.

The most important feature is that the spectra consist of a superposition of a paramagnetic, singlet for $LaFe_{1-x}Cr_xO_3$ or doublet for $Fe_{2-2x}Cr_{2x}O_3$ respectively, and enlarged magnetic sextet below the magnetic ordering transition temperature as presented in figure 9. We can notice that similar behavior was previously observed in randomly canted ferrite $Li_{0.5+x/2}Ti_xFe_{2.5-3x/2}O_4$, $Li_{0.5}Fe_xAl_{2.5-x}O_4$, frustrated spinel $ZnCr_{2x}Ga_{2-2x}O_4$ and mixed fluoride $Fe_{1-x}Cr_xF_3$.[29-32]

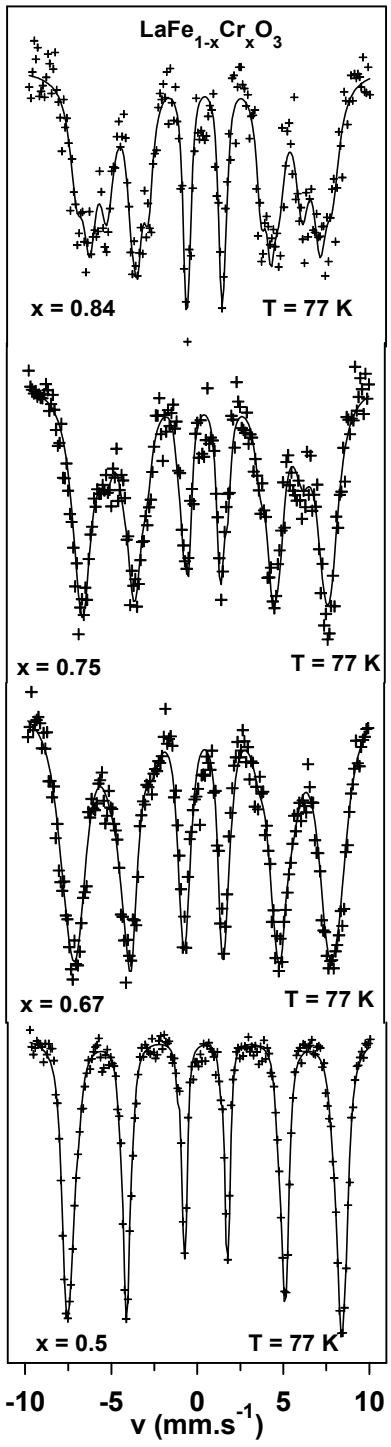

FIG. 10: Mössbauer spectra at 77 K for the samples $LaFe_{0.5}Cr_{0.5}O_3$, $LaFe_{0.33}Cr_{0.67}O_3$, $LaFe_{0.25}Cr_{0.75}O_3$ and $LaFe_{0.16}Cr_{0.84}O_3$.

For all the samples, strong relaxation effects and perturbed spectra occur over a certain range of temperature below T_N as shown in figure 10. The relaxation phenomena observed by Mössbauer spectroscopy can be associated with blocking process of spin clusters in superparamagnetic state with different height energy barriers. Almost all the spin directions are probably allowed and the order does not retain the memory of the initial antiferromagnetic order.

Table 2: Hyperfine parameters at 77 K for different chromium concentration in the case of $LaFe_{1-x}Cr_xO_3$ solid solution. Γ is the linewidth at halfheight, ε the quadrupolar splitting H_{hf} the mean hyperfine field.

x	δ ($mm.s^{-1}$)	Γ ($mm.s^{-1}$)	ε ($mm.s^{-1}$)	H_{hf} (kOe)
0.25	0.47	0.28	0.01	530
0.50	0.47	0.55	0.03	492
0.67	0.47	0.67	0.04	457
0.75	0.48	0.71	0.05	426
0.84	0.45	0.78	0.08	408

Table 3: Hyperfine parameters at 77 K for different chromium concentration in the case of $Fe_{2-2x}Cr_{2x}O_3$ solid solution.

x	δ ($mm.s^{-1}$)	Γ ($mm.s^{-1}$)	ε ($mm.s^{-1}$)	H_{hf} (kOe)
0.25	0.49	0.50	0.01	521
0.50	0.48	0.55	0.08	519
0.75	0.49	0.60	0.11	505
0.875	0.49	0.67	0.16	428

III. DISCUSSION

From hysteresis loop measurements we have shown previously that the remanent magnetization M_r and the coercive field H_c for $LaFe_{1-x}Cr_xO_3$ present unusual behavior.[10,11] The remanent magnetization M_r decreases quasi linearly when T increases while the variation of H_c vs. temperature presents a minimum value H_{c_1} at a temperature T_1 and a maximum H_{c_2} at T_2 for x>0.5. At low temperature an important increase of H_c occurs, depending on the height of the energy barriers. The temperature dependence of coercive field depends on a thermally activated process, which can be related to energy barriers occurring between metastable magnetic states induced by frustration. Below T_1 and above T_2, the temperature dependence of the coercive field can be fitted by an exponential law $H_c(T) \approx H_{c_0} e^{-E_x T}$ as has been signaled for semi-disordered spinel.[31,33] In the mixed systems $LaFe_{1-x}Cr_xO_3$ and $Fe_{2-2x}Cr_{2x}O_3$, the presence of both Fe and Cr in the crystal lattice leads to frustration phenomena because of the antagonist characters of iron ion Fe^{3+} and the chromium ion Cr^{3+}. As demonstrated by the Mössbauer effect measurements a random distribution of Fe and Cr in the lattice is expected, we can then expect a distribution of canting angles of the antiferromagnetic network related to the local concentration of Fe (Cr) ions. By examining the shape of the temperature dependence of M_{sat} we can explain its variation by considering the existence of many distributed weak ferromagnetic components anti-ferromagnetically coupled. According to the Néel theory for the ferrimagnetism,[34] we consider two weak ferromagnetic components M_1 and M_2, with concentrations N_1 and N_2 respectively. The values of M_1, M_2, N_1 and N_2, depend on the chromium concentration. If $N_1M_1 \geq N_2M_2$, then at T=0 $M(T) \neq 0$ and begin to increase with temperature, passes trough a maximum and falls down to zero at the transition temperature, which is the case of $LaFe_{0.5}Cr_{0.5}O_3$. When $N_1M_1 \approx N_2M_2$ the M(T) curve decreases regularly with increasing temperature and presents a slope equal to zero at the transition temperature. We think that may be the case of $LaFe_{0.25}Cr_{0.75}O_3$. The residual part of $M_{sat}(T)$ varies linearly with temperature until the room temperature. This behavior can be explained by the presence of magnetic spin clusters as confirmed by the hysteresis loop measurements. The curves of $M_{sat}(T)$ for $Fe_{0.25}Cr_{1.75}O_3$ and $Fe_{0.5}Cr_{1.5}O_3$ show that the initially predominant component is opposite to the magnetic field while in the case of the $FeCrO_3$ the curve shows a compensation point near 80 K.

Zero field cooled (ZFC) and field cooled (FC) magnetization at low field have been carried out. The ZFC curves of the temperature dependence of the magnetization were obtained after the samples had been cooled in zero field from room temperature and measured increasing the temperature, while the FC curves were obtained after the samples had been cooled in applied field from room temperature. The ZFC and FC magnetization measurements exhibit strong irreversibilities for all the samples studied. Since the applied field H_a is less than the coercive field, these irreversibilities in ZFC-FC curves could only be the consequence of the variation in the hysteresis loop with the temperature rather than spin-glass-like behavior. The sharp decrease in magnetization curves is characteristic of a change in the magnetic structure. So all those observations confirm that the magnetic moments must be ordered in non-collinear manner, i.e. the magnetization has an antiferromagnetic component plus a ferromagnetic component. The observed increase of the coercive field with decreasing temperature can explain, in terms of the difficulties of motion of domain walls, the anomalies which appear at very low temperature in the ZFC-FC curves. We can note that anomalous in temperature dependence of the magnetic moment of $Fe_{2-2x}Cr_{2x}O_3$ for $0.1 \leq x \leq 0.5$ has been observed and

explained by antiparallel orientation of the mean weakly-ferromagnetic moments of Fe^{3+} and Cr^{3+} ions.[28]

For all the studied samples the paramagnetic Curie temperature θ_p is negative indicating the existence of antiferromagnetic interactions. The magnetic ordering temperatures obtained from the jump located below the linear part of $\chi^{-1}(T)$ are different from those determined from Mössbauer spectroscopy, as it will be discussed later. When x<0.5, i.e. high concentration of iron, the behavior of χ^{-1} (T) is more complicate. The evolution of the inverse susceptibility curve shows a very large magnetic transition where short-range order exists resulting from the complex arrangement of ions in the matrix. For more comprehension we plot in figure 11 the variation of χT versus T.

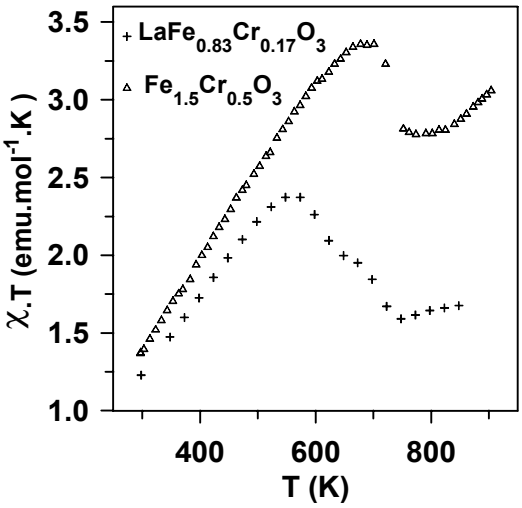

FIG. 11: Variation of χT vs. temperature for $LaFe_{0.83}Cr_{0.17}O_3$ and $Fe_{1.5}Cr_{0.5}O_3$.

The χT diagrams are characteristic of competition between ferromagnetic and antiferromagnetic interactions. Since the magnetic structure of α-Fe_2O_3 and Cr_2O_3 are described respectively by the following magnetic modes[28] :

$$L_{\alpha-Fe_2O_3} = M_1 + M_2 - M_3 - M_4$$

$$L_{Cr_2O_3} = M_1 - M_2 + M_3 - M_4$$

We can assume that frustration results from the competition between the two modes.

The Mössbauer effect has proved its utility in the study of dynamical properties of spin systems. The spin fluctuations can modulate the shape of the Mössbauer spectra when the fluctuation rate is comparable to the nuclear procession frequency. The shape in the presence of these fluctuations can be computed using perturbation methods or the stochastic model in spin fluctuations and the comparison of the calculated spectrum with the experimental data gives rise to more information about the spin transition modes. The variation of the spectrum shape with the chromium concentration depends on the relaxation condition. With increasing the temperature, a paramagnetic component appears superimposed to the magnetic hyperfine pattern. The relative population in the paramagnetic state increases with the temperature, until T_N where the spectrum is completely paramagnetic. The paramagnetic population detected by Mössbauer spectroscopy in the magnetic transition region may be due either to a paramagnetic short-range order, or to fraction of magnetically ordered entities, depending on the local composition in the lattice, that can behave superparamagnetically. The Néel temperature estimated by Mössbauer spectroscopy is smaller than that obtained from magnetization measurements. Relaxation effects could be responsible of the shift via spin-spin relaxation involving the nuclear levels as also observed in several frustrated systems.[35] In addition, the presence of short-range magnetic order can perturb the T_N determination from Mössbauer spectroscopy. For $Fe_{0.25}Cr_{0.75}O_3$, some typical spectra are shown in figure 12.

At T = 4.2 K the spectrum is well-defined sextuplet. When the temperature increases the sextuplet's shape deviates towards that of one largely influenced by relaxation phenomena, which render the determination of hyperfine parameters difficult. This line broadening in Mössbauer spectra can be caused by a change in the near neighbor environment which be different for iron ions at equivalent crystal sites. This fact can also be related to complex antiferromagnetic structures as has been shown by neutron experiments.[26,36] On the other hand the direction of magnetization changes rapidly due to thermal energy and frustration. We can also assume that the complex Mössbauer spectra result from the multitude of possible environment for an iron ion in the mixed $Fe_{2-2x}Cr_{2x}O_3$. The hyperfine field H_{hf} will depends on the number and the type of cations neighbors. When T increases there is a decrease of H(T) to zero, which is indicative of a magnetic transition.

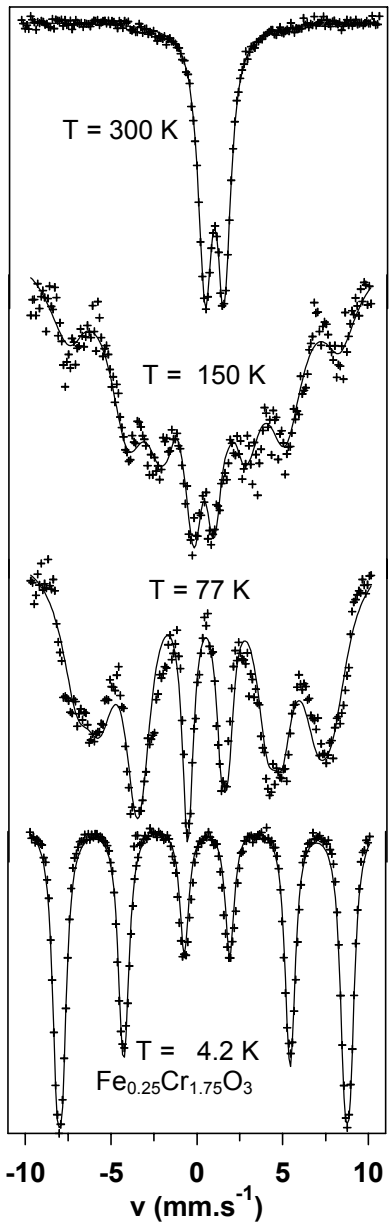

FIG. 12 : Mössbauer spectra of $Fe_{0.25}Cr_{1.75}O_3$ at different temperatures.

On the basis of the measurements, it is clear that the transition from paramagnetism towards the non-collinear antiferromagnetism takes place through a large domain of temperature. Moreover, above T_N, we observe the existence of hysteresis loop, and small remanent magnetization, which doesn't vanish until the paramagnetic state. This behavior can be explained as follows:

At high temperature, the spins relax independently, in spite of the presence of magnetic interactions. Then, as short range magnetic correlations appear when the temperature decreases, one can suppose the existence of small spin clusters, resulting from the frustration mechanism induced by the presence of both Fe and Cr ions. The growth of these spin clusters at low temperature leads to coalescence and finally to the creation of an infinite cluster. Finally, we propose the magnetic phase diagrams for frustrated $LaFe_{1-x}Cr_xO_3$ and $Fe_{2-2x}Cr_{2x}O_3$ systems in figures 13 and 14. For x=0 and x=1 a long-range antiferromagnetic order is observed. The substitution of iron by chromium perturbs this antiferromagnetic order. Different magnetic regions could be distinguished. With increasing x, the initial antiferromagnetic state is progressively perturbed and uncompensated weak ferromagnets, antiferromagnetically coupled and antiferromagnetic clusters are formed within the antiferromagnetic matrix.

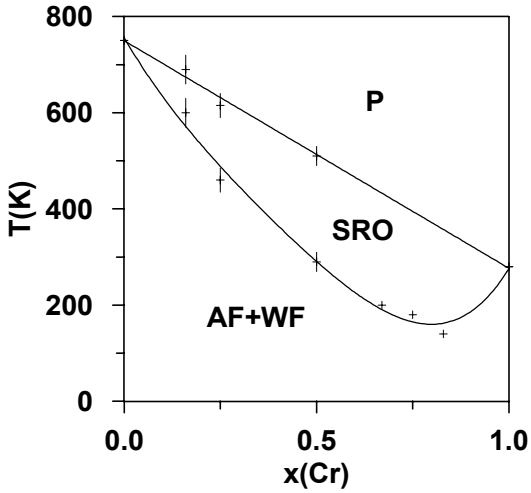

FIG. 13 : Magnetic phase diagram of $LaFe_{1-x}Cr_xO_3$ system. AF: antiferromagnetic structure; P: paramagnetic regime; WF: weak ferromagnetic component; SRO: short range order; MS: modulated structure

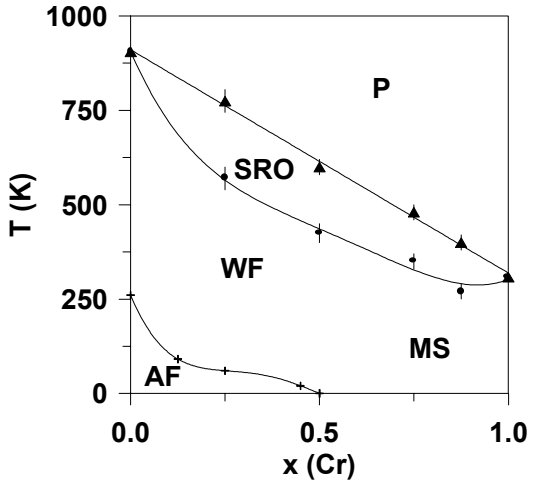

FIG. 14 : Magnetic phase diagram of $Fe_{2-2x}Cr_{2x}O_3$ system.

The Néel temperature is determined using the magnetization measurements, the Mössbauer spectroscopy and the d.c. magnetic susceptibility.

IV. CONCLUSION

Analyses of various data taken in two different mixed oxides permit us to investigate their magnetic properties. The studied systems present non-collinear antiferromagnetic structures. The magnetization measurements indicate the existence of many distributed weak ferromagnetic components. Strong relaxation effects in the Mössbauer spectra occur over a certain range of temperature below T_N probably due to spin-spin and spin-lattice relaxation mechanisms. Short-range magnetic correlations appear when the temperature decreases and small spin clusters can exist inducing the combination of a pure paramagnetic component and a magnetic sextet. A qualitative description of the experimental magnetic phase diagrams is made in terms of perturbed antiferromagnetic matrix and clusters taking into account the performance of the different techniques used in this work.

[1]G.J. Nieuwenhuys, B.H. Verbeek and J.A. Mydosh, J. Appl. Phys. **50**, 1685 (1979).
[2]Y. Ishikawa, M. Arai, N. Saito and M. Kohgi, J. Magn. Magn. Mater. **31-34**, 1381 (1983).
[3]S.K. Burke and B.D. Rainford, J. Phys. F : Met. Phys. **13**, 441 (1983)
S.K. Burke and B.D. Rainford, J. Phys. F : Met. Phys. **13**, 451 (1983)
S.K. Burke and B.D. Rainford, J. Phys. F : Met. Phys. **13**, 471 (1983)
[4]T. Brückel, W. Praud and P. Convert, J. Phys. C : Solid State Phys. **20**, 2565 (1988).
[5]H. Aruga, A. Ito, H. Wakabayashi and T. Goto, J. Phys. Soc. Jap. **57**, 2636 (1988).
A. Ito, H. Aruga, M. Kikushi, Y. Syono and H. Takei, Solid State Comm. **66**, 475 (1988).
A. Ito, H. Kawamo, H. Yoshizawa and K. Motoya, J. Magn. Magn. Mater. **104-107**, 1637 (1992)
H. Aruga Katori, T. Goto, S. Ebii and A. Ito, J. Magn. Magn. Mater. **104-107**, 1639 (1992).
[6]A. Avramescu, B. Seling, C. Schinger, A. Ehmann, S. Kemlersack and M. Rosenberg, J. of Alloys & Compounds **240**, 170 (1996)
[7]MM. Kumar, S. Srintah, G.S. Kumar and S.V. Suryanarayana **188**, 203 (1998)
[8]Y. Doi and Y. Hinatsu, J. Phys. Condens. Matter. **11**, 4813 (1999)
[9]M. Hervieu, A. Barnabe, C. Martin, A. Maignan, F. Dassay and B. Raveau, Eur. Phys. J. B **8**, 31 (1999)
[10]A. Belayachi, M. Nogues, J.L. Dormann and M. Taibi, Eur. J. Solid State Inorg. Chem. **33**,1039 (1996)
[11]A. Belayachi, E. Loudghiri, M. ElYamani, M. Nogues, J.L. Dormann and M. Taibi, Ann. Chim. Sci. Mat. **23**, 297 (1998)
[12]R. Street and B. Lewis, Phil. Mag. **1,** 663 (1956)
[13]S. Foner, Physical Review **130** (1), 183 (1963)
[14]G.W. Pratt Jr and P.T. Bailey, Phys. Rev. **131**, 1923 (1963).
[15]L.M. Corliss, J.M. Hastings, R. Nathans and G. Shirane, J. Appl. Phys. **36** (3), 1099 (1965)
[16]F. Van Der Woode, Phys. Stat. Sol. **17**, 417 (1966)
[17]T. Ruskov, T. Tomov and S. Georgiev, Phys. Stat. sol. (a) **37,** 295 (1976)
[18]Ö.F. Bakkaloglu and M.F. Thomas, J. Magn. Magn. Mater. **104-107,** 1921 (1992)
[19]R.P. Eischens and P.W. Selwood, J. American Chem. Soc. **69**, 2698 (1947)
[20]C.P. Poole Jr and J.F. Itzel Jr., J. of Chemical Physics **41** (2), 287 (1964)
[21]C. Marcilly and J. Villaine, C. R. Acad. Sc. Paris **t. 265**, 367 (7 Aout 1967)
[22]C.J. Carman and W.J. Kroenke, J. of Physical Chemistry **72** (7), 2562 (1968)
[23]F.S. Stone and J.C. Vickerman, Trans. Faraday Soc. GB **67** N°518, 316 (1971)
[24]J.M.D. Coey and G.A. Sawatzky, J. Phys. C : Solid State Physics **4**, 2386 (1971)
[25]V.V. Viktorov, Phys. Stat. Sol. (b) **174**, 529 (1992)
[26]D. Cox, W. Takei and S. Shirane, J. Phys. Chem. **24**, 405 (1963)
[27]J.K. Srivastava and R.P. Sharma, Phys. Stat. Sol. **35**, 491 (1969)
[28]G.P. Vorob'ev, A.M. Kadomtseva, A.S. Moskvin, Yu.F. Popov and V.A. Timofeeva, Phys. Solid State **39** (1), 97 (1997)
[29]D. Fiorani, S. Viticoli, J.L. Dormann, J.L. Tholence and A.P. Murani, Phys. Rev. B. **30**, 2776 (1984)
[30]J.L. Dormann, M. EL Harfaoui, M. Nogues and J. Jove, J. Phys. C: Solid State Phys. **20**, L 161 (1987).
[31]J. Maknani, J.L. Dormann, M. Nogues, F. Varret and J. Teillet, Hyperfine Interactions **54**, 603 (1990).
[32]M. Lahlou Mimi, Y. Pennec, J.M. Bassat, M. Leblanc and J.M. Grenèche, J. Magn. Magn. Mater. **129**, 289 (1994).
[33]G.T. Bhandage, A. Belayachi, M. Nogues, G. Villers, J.L. Dormann and H.V. Keer, J. Magn. Magn. Mater. **166**, 1921 (1996).
[34]A. Herpin, in "Théorie du magnétisme", Institut National de Sciences et Techniques, Saclay p 625 (1968)
[35]J. L. Dormann and M. Nogues, J. Phys. C: Condens. Matter. **2**, 1223 (1990).
[36]M. Hamdoun, A. Wiedenmann, J.L. Dormann, M. Nogues, and J. Rossat-Mignod, J. Phys. C: Solid State Phys. **19**, 1783 (1986)